Walter et al., http://www.jcb.org/cgi/content/full/jcb.200907018/DC1

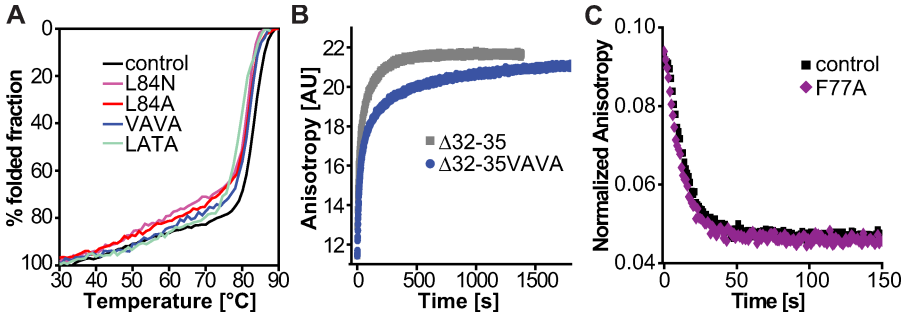

Figure S1. **Synaptobrevin mutants form stable complexes, and fast assembly requires interaction of the first four N-terminal layers.** (A) Both C- and N-terminal mutants form stable complexes and maintain similar melting temperatures as revealed by CD spectroscopic characterization. (B) Binding of a deletion mutant of syb-2 (Δ32–35) to the ΔN complex. The deletion mutant carried a deletion of layers −7 and −6. Mutating layers −5 and −4 (VAVA) in the deletion mutant caused a further slowdown of binding. The concentration of syb-2 was 100 nM, and the concentration of the ΔN complex was 6 µM (therefore binding was much faster here than in Fig. 2 A, in which the concentration of the ΔN complex was only 500 nM). AU, arbitrary unit. (C) Synaptobrevin carrying the F77A mutation can displace the synaptobrevin fragment from the ΔN complex. 100 nM of the ΔN complex was incubated with 500 nM of WT synaptobrevin or the mutant Syb F77A (cytoplasmic domain, aa 1–96). The Alexa Fluor 488–labeled synaptobrevin fragment (Syb49–96) was quickly displaced upon the addition of synaptobrevin, indicating normal binding (Pobbati et al., 2006; Wiederhold and Fasshauer, 2009).

THE JOURNAL OF CELL BIOLOGY

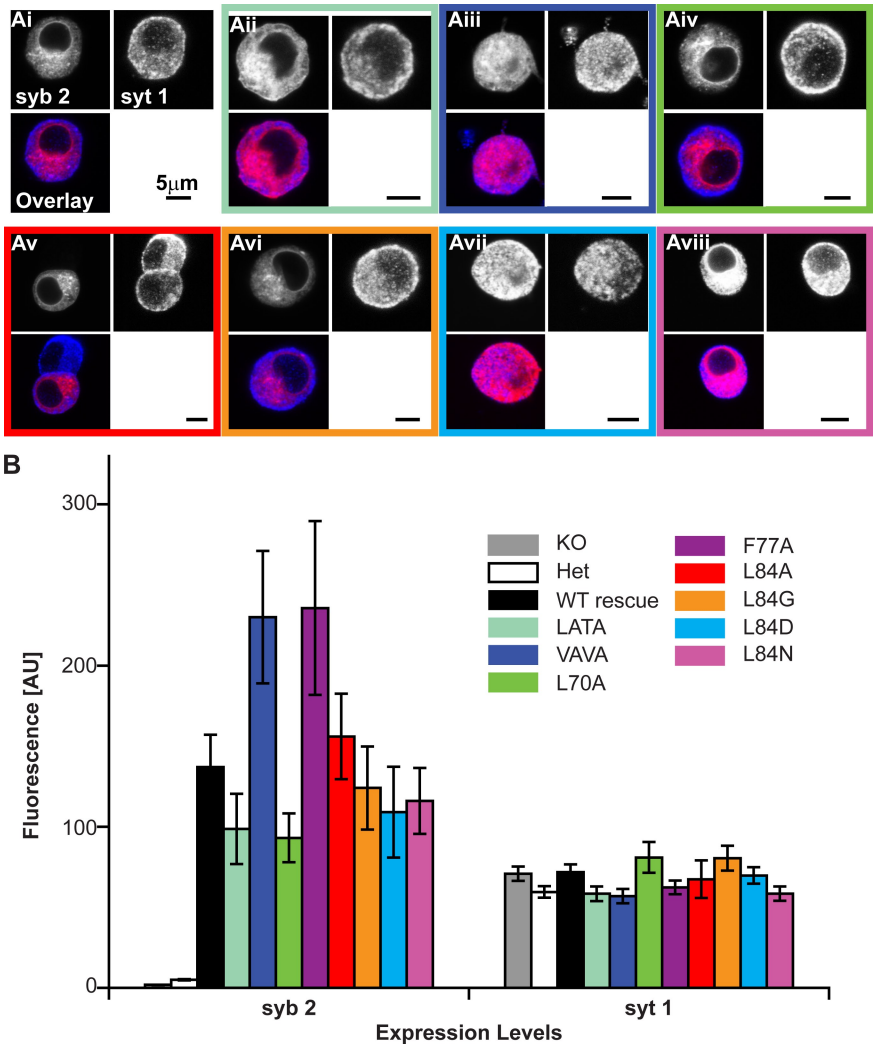

Figure S2. **Localization and expression levels were tested by quantitative immunostaining.** (A) Confocal images of fixed chromaffin cells stained for syb-2 (visualized by secondary antibody bearing Alexa Fluor 546) and syt-1 (visualized by Alexa Fluor 647). (Ai–Aviii) Images of double knockout cells expressing syb-2 WT protein (WT rescue; Ai) or LATA (Aii), VAVA (Aiii), L70A (Aiv), L84A (Av; note that this image contains two attached cells of which one expresses the virus and is positive for syb-2; the uninfected cell is negative for synaptobrevin but positive for syt-1), L84G (Avi), L84D (Avii), and L84N (Aviii) mutations. Each image contains three representations of the same field of view: first channel (top left), syb-2; second channel (top right), syt-1; and third channel (bottom left), overlay. (B) Quantification of expression levels by fluorescence intensity (integrated fluorescence over the whole cell). Mean ± SEM is shown. AU, arbitrary unit; KO, knockout.

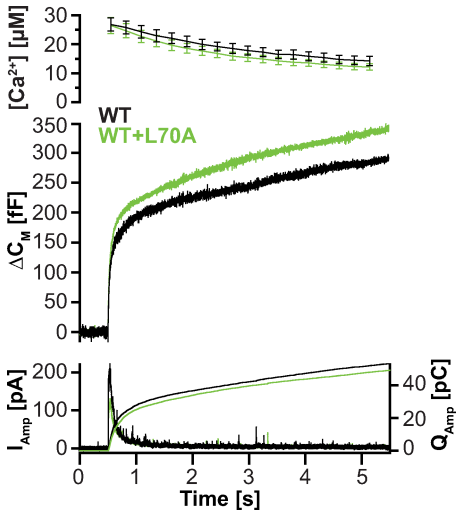

Figure S3. **The layer 4 mutant (L70A) does not act as a dominant negative on a WT background.** Mean secretory response in Ca^{2+}-triggered release is unaffected by expression of the layer 4 mutant in WT cells. Mean ± SEM of Ca^{2+} levels is shown (WT cells, *n* = 6 cells; and WT + L70A, *n* = 13 cells).

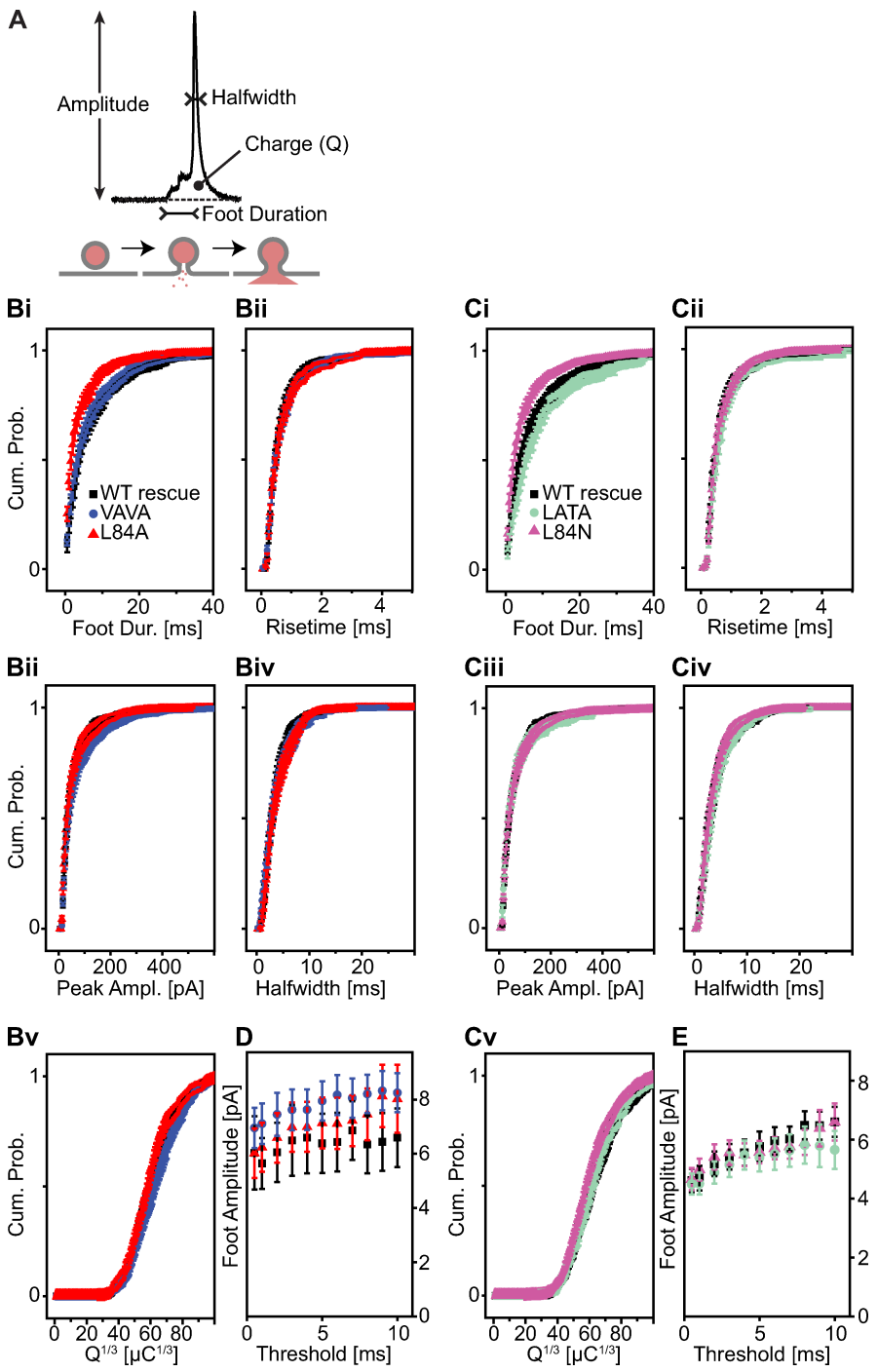

Figure S4. **Single spike analysis shows that fusion pore stability is selectively and significantly affected by C- but not N-terminal SNARE complex destabilization.** (A) An amperometric spike. The shape of the spike is characterized by its amplitude, its 50–90% rise time, half-width, its charge (Q; a measure of neurotransmitter content in one vesicle), and the cubic root of the charge (proportional to the vesicle diameter). Efflux of neurotransmitter from a vesicle through the fusion pore before full collapse of the vesicle produces a prespike foot. (B) Cumulative probability distribution of amperometric spike parameters and binned data showing mean and SEM of cell distributions. (Bi and Ci) Foot duration (Dur.). (Bii and Cii) Rise time. (Biii and Ciii) Peak amplitude (Ampl.). (Biv and Civ) Half-width. (Bv and Cv) Cubic root of peak charge. (D and E) Amplitude of prespike feet as a function of a selected minimal duration (threshold) for feet analyzed. Overlapping values of the prespike foot amplitude indicate that fusion pore conductance is unaffected by synaptobrevin mutants and that foot shapes are conserved over a broad range of feet length (same cells as in Fig. 6). Mean ± SEM is shown.

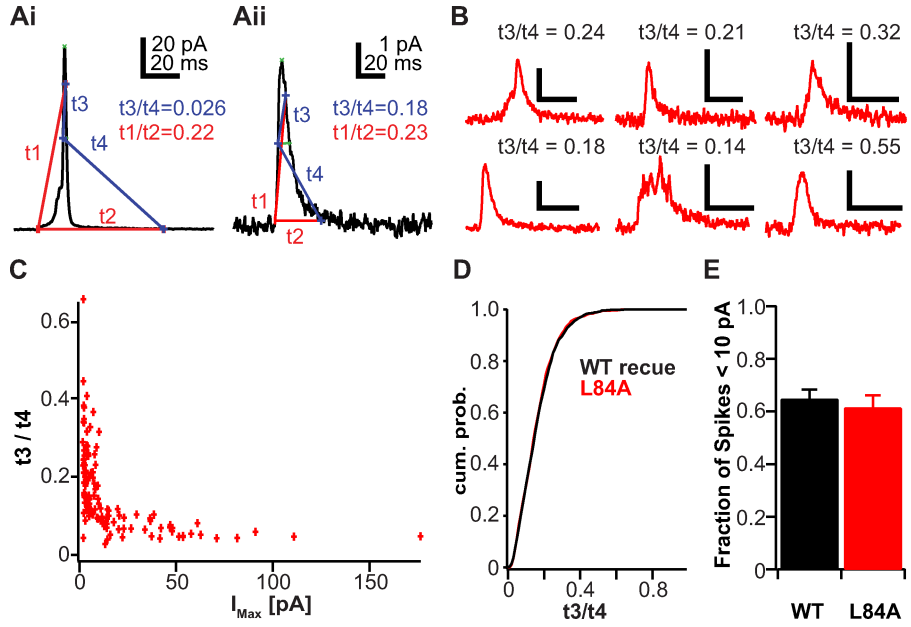

Figure S5. **Attempt to detect SAFs in embryonic mouse chromaffin cells.** (A) Ai and Aii show two spikes, a large one with a prominent prespike foot (Ai) and a smaller one (Aii). Two criteria were applied: t1 and t2 are two different duration measures, both starting at the point where the signal departs by more than 1× root mean square of the noise above baseline. The end point of t1 was defined as the mean spike amplitude between the two time boundaries defined by the half-way points between peak amplitude and baseline. The end point of t2 is defined as the time when the signal returned to within 1× root mean square of the baseline. These definitions were taken from Wang et al. (2006), where the quotient t1/t2 was proposed as a useful criterion for detecting SAFs. However, in our case, the two spikes (Ai and Aii) result in rather similar t1/t2 quotients in spite of very dissimilar amplitudes and shapes. The reason is that the large spike in Ai has a rather long prespike foot, which enters into the calculation of t1. Therefore, we defined two new duration measures t3 and t4, whose end points are identical to those of t1 and t2, but with the common start point at the time the spike exceeds half its maximal amplitude. Because most prespike feet were smaller than half of the maximal amplitude, the t3/t4 quotient might be a better measure for the shape of the spike itself when prespike feet are of longer duration. (B) A collection of small events with their t3/t4 quotient. For most of the events, it is hard to determine off hand whether they are SAFs or just small spikes originating far away from the recording electrode. The exception is the second to last event, which can hardly be interpreted as anything but an SAF. However, such events were infrequent; most were more transient. (C) Plot showing the dependency of the t3/t4 quotient on the maximal peak amplitude of the event for all events detected from a single cell. The plot clearly shows that events <10 pA have a larger t3/t4 ratio than larger spikes. This might indicate a more rectangular shape of small events; however, the larger ratio might also be explained by a smaller signal to noise ratio of smaller events, which displaces the end point of t3 and t4 to earlier times. Vertical bar, 2 pA; horizontal bar, 40 ms. (D) Cumulative probability (cum. prob.) distribution of the t3/t4 criterion is unchanged in the L84A mutant compared with WT rescue. (E) The fraction of events with amplitude <10 pA was unchanged in the L84A mutant compared with WT rescue. Mean ± SEM is shown (cell means: WT rescue, *n* = 11; and L84A-expressing cells, *n* = 12).

Table S1. **Details of parameters obtained by kinetic analysis of capacitance responses after regional synaptobrevin destabilization**

Condition/ construct tested	RRP size	τ (RRP)	SRP size	τ (SRP)	Sustained rate	*n*
	fF	*ms*	*fF*	*ms*	*fF/s*	
WT rescue	61.4 ± 6.60	24.4 ± 3.53	54.6 ± 10.7	174 ± 23.8	18.0 ± 3.00	21
LATA	28.8 ± 5.52	22.4 ± 5.57	22.2 ± 5.94	286 ± 40.6	9.24 ± 2.32	20
VAVA	34.5 ± 7.01	27.7 ± 5.50	25.0 ± 5.97	258 ± 39.6	11.3 ± 2.17	29
WT rescue	65.3 ± 13.4	19.5 ± 3.08	54.5 ± 10.0	201 ± 31.3	17.0 ± 2.75	19
L84A	43.5 ± 8.99	40.0 ± 5.29	55.0 ± 11.3	291 ± 49.0	18.9 ± 3.18	25
WT rescue	57.1 ± 9.70	17.0 ± 2.14	47.7 ± 7.27	153 ± 30.6	21.5 ± 2.70	24
L84D	24.2 ± 6.44	35.6 ± 10.3	47.8 ± 9.23	330 ± 51.5	20.7 ± 1.96	19
L84N	30.3 ± 6.68	38.8 ± 7.26	82.3 ± 12.4	284 ± 28.1	34.0 ± 10.9	23
L84G	26.8 ± 6.27	31.6 ± 6.75	46.1 ± 9.34	359 ± 72.5	14.0 ± 3.14	19

Kinetic values of capacitance recordings from mouse embryonic adrenal chromaffin cells isolated from syb-2/cellubrevin double knockout animals and expressing WT syb-2 or various mutants (as indicated in left column). *n* gives the total number of cells included in the analysis. The number of observations of the two vesicle pools (SRP and RRP) and their fusion time constant can be lower because not every cell displayed both kinetic components.

References

Pobbati, A.V., A. Stein, and D. Fasshauer. 2006. N- to C-terminal SNARE complex assembly promotes rapid membrane fusion. *Science*. 313:673–676. doi:10.1126/science.1129486

Wang, C.T., J. Bai, P.Y. Chang, E.R. Chapman, and M.B. Jackson. 2006. Synaptotagmin-Ca2+ triggers two sequential steps in regulated exocytosis in rat PC12 cells: fusion pore opening and fusion pore dilation. *J. Physiol.* 570:295–307.

Wiederhold, K., and D. Fasshauer. 2009. Is assembly of the SNARE complex enough to fuel membrane fusion? *J. Biol. Chem.* 284:13143–13152. doi:10.1074/jbc.M900703200